GEOPHYSICS, VOL. 72, NO. 5 (SEPTEMBER-OCTOBER 2007); P. SM169–SM175, 5 FIGS.
10.1190/1.2738553

Application of the nearly perfectly matched layer in acoustic wave modeling

Wenyi Hu[1], Aria Abubakar[1], and Tarek M. Habashy[1]

ABSTRACT

In this work, we successfully applied an alternative formulation of the perfectly matched layer (PML), the so-called nearly PML (NPML), to acoustic wave propagation modeling. The NPML formulation shows great advantages over the standard complex stretched coordinate PML. The NPML formulation deviates from the standard PML through an inexact variable change, but this fact only affects the wave behavior in the NPML layer, which is outside the region of interest. The equivalence of the wave-absorbing performance between these two PML formulations (the standard complex stretched coordinate PML formulation and the NPML formulation) in 3D Cartesian coordinates for acoustic wave propagation modeling is proved mathematically in this work. In time-domain methods, the advantages of the NPML over the standard PML were explained by both the analytical analysis and the numerical simulations in terms of implementation simplicity and computational efficiency. The computation time saving is up to 17% for the 2D example used in this work. For 3D problems, this computational saving is more significant. After theoretically analyzing the numerical reflections from the NPML and the standard PML, we concluded that these two PML formulations have exactly the same performance, even after spatial discretization. This conclusion is validated by numerical experiment. Finally, we tested the NPML in the Marmousi velocity model and found its wave-absorbing rate is high enough, even for this realistic structure.

INTRODUCTION

To simulate wave propagations in an unbounded domain, absorbing boundary conditions (ABCs) have to be applied to truncate the computational domain to minimize artificial reflections. There are a variety of ABCs available, including field extrapolation, impedance condition, one-way wave equation approximation, absorbing material boundary condition, etc.

Among these approaches, the one-way wave equation, introduced by Engquist and Majda (1977) and Mur (1981), has been widely used. However, this absorbing boundary condition works effectively only for normally or nearly normally incident waves. The artificial reflections introduced by this one-way wave equation absorbing boundary condition are highly dependent on the incident angles.

A very effective absorbing boundary condition, the perfectly matched layer (PML), was originally developed by Bérenger (1994). The PML is an absorbing material boundary condition. In this approach, the computational domain is wrapped by the absorbing material, which is designed to absorb the outgoing waves. In comparison with the one-way wave equation absorbing boundary condition, the PML has a much better wave-absorbing performance because, with the PML absorbing boundary condition, the waves do not necessarily have to be incident at normal incidence angle to achieve a high wave-absorbing rate.

Since the original split-field PML was proposed, many alternative formulations of the PML have been developed to simplify the implementation (Chew and Weedon, 1994; Sacks et al., 1995; Roden and Gedney, 2000). The original PML was also extended to 3D (Katz et al., 1994; Bérenger, 1996) and dispersive anisotropic medium applications (Gedney, 1996). These PML formulations can be classified into two categories. (1) The resulting partial differential equations (PDEs) in the PML regions are in the same form as the original governing equations in the physical medium, e.g., complex stretched coordinate PML (Chew and Weedon, 1994). (2) The resulting PDEs in the PML regions are modified, thus different from the governing equations in the physical medium, e.g., the split-field PML, convolution PML (Bérenger, 1994; Roden and Gedney, 2000).

Cummer (2003) developed another novel PML formulation, referred to as the nearly perfectly matched layer (NPML). This alternative PML formulation has been shown to possess some valuable advantages over the standard PML formulations in implementation

Manuscript received by the Editor November 27, 2006; revised manuscript received February 12, 2007; published online August 23, 2007.
[1]Schlumberger-Doll Research, Cambridge, Massachusetts. E-mail: whu@boston.oilfield.slb.com; aabubakar@boston.oilfield.slb.com; thabashy@ridgefield.oilfield.slb.com.

simplicity and computational efficiency for time-domain methods (Hu and Cummer, 2004; Bérenger, 2004). The NPML does not modify the original form of the governing equations in any linear media. Compared with the standard complex stretched coordinate PML, the NPML uses fewer auxiliary variables and fewer extra ordinary differential equations. Furthermore, the implementation of the NPML in complex configurations is very straightforward (Cummer, 2003).

The derivation of the NPML formulation was based initially on an inexact variable change when the NPML parameter is spatially varying, as it would be in a practical implementation (Cummer, 2003). However, using different approaches, Hu and Cummer (2004) and Bérenger (2004) proved that these two PML formulations are mathematically equivalent in 2D Cartesian coordinates for electromagnetic wave propagations. Even for spatially varying NPML conductivity profiles, the electromagnetic waves reflected from the NPML and the standard PML layers are identical, and thus the implementation simplicity of the NPML does not require a trade-off in exactness or performance. After that, the NPML was employed to solve various practical problems in electromagnetics (Cummer, 2004; Ramadan, 2005; Hu and Cummer, 2006).

In this work, we apply the NPML absorbing boundary condition to acoustic wave propagation modeling and extend the NPML to 3D Cartesian space for the finite-difference time-domain method (FDTD). We show that the advantages of the NPML are maintained in acoustic wave propagation modeling and that the computational saving is more significant in 3D cases because more auxiliary state variables and more ordinary differential equations are saved. Then, we prove the mathematical equivalence between the NPML and the standard PML in 3D Cartesian coordinates.

We further rigorously analyze the numerical reflections from the NPML and the standard PML. Finally, we apply the NPML on a realistic acoustic model and investigate its wave-absorbing performance in this complicated configuration.

FORMULATIONS

The formulation of the NPML is similar to the standard complex stretched coordinate PML formulation (Chew and Weedon, 1994). The advantage of the complex stretched coordinate technique over the original split-field technique (Bérenger, 1994) is obvious in implementation because the former preserves the structure of the original governing equation form in the whole computational domain (the physical medium region and the PML layers). Furthermore, this approach can be easily extended to curvilinear coordinate systems and results in a better wave-absorbing performance than the split-field PML (Collino and Monk, 1998). Without losing any of these advantages, the NPML is even simpler to implement and more computationally efficient than the standard complex stretched coordinate PML.

Governing equations

The governing equations describing acoustic wave propagations are given by (Fokkema and van den Berg, 1993)

$$\nabla p + \rho \frac{\partial \mathbf{v}}{\partial t} = \mathrm{f}, \tag{1}$$

$$\nabla \cdot \mathbf{v} + \frac{1}{\lambda}\frac{\partial p}{\partial t} = q, \tag{2}$$

where p is the acoustic pressure (Pa), $\mathbf{v}$ is the particle velocity (m/s), $\mathbf{f}$ is the volume density of the body force (N/m^3), q is the volume density of the injected volume rate (s^{-1}), ρ is the volume density of mass (kg/m^3), λ is the Lamé modulus, and t is the time variable. In equations 1 and 2, the vectors are denoted by boldface symbols.

The governing equations can be written in the frequency domain with the time factor $\exp(j\omega t)$, where $j^2 = -1$ and ω is the angular frequency, as follows:

$$\frac{\partial p}{\partial \alpha} + j\omega\rho v_\alpha = f_\alpha, \tag{3}$$

$$\frac{\partial v_x}{\partial x} + \frac{\partial v_y}{\partial y} + \frac{\partial v_z}{\partial z} + \frac{1}{\lambda} j\omega p = q, \tag{4}$$

where $\alpha \in \{x, y, z\}$.

Standard PML and NPML formulations

In the complex stretched coordinate approach (Chew and Weedon, 1994), the standard PML formulation is written as

$$\frac{\partial p}{\gamma_\alpha \partial \alpha} + j\omega\rho v_\alpha = f_\alpha, \tag{5}$$

$$\frac{\partial v_x}{\gamma_x \partial x} + \frac{\partial v_y}{\gamma_y \partial y} + \frac{\partial v_z}{\gamma_z \partial z} + \frac{1}{\lambda} j\omega p = q. \tag{6}$$

Here, γ_α is the complex stretched coordinate factor, which is given by

$$\gamma_\alpha = 1 - j\eta_\alpha/\omega, \tag{7}$$

where η_α is the PML decay factor and $\alpha \in \{x, y, z\}$.

Theoretically, the wave impedance of the physical medium and the PML is perfectly matched (Bérenger, 1994). Thus, the wave transmission from the physical medium region to the PML region is perfect and reflectionless for all incident angles and the PML layer thickness can be as thin as required to save the computational expense if the decay factor η is large enough. However, this is not practically true because the discontinuity in the PML decay factor η at the PML/non-PML interface introduces numerical reflections, which prevents the PML from being a perfect absorbing boundary condition. Consequently, when we determine the thickness of the PML layer, the trade-off between computational cost and computational accuracy must be considered carefully. Usually, the decay factor η varies gradually from 0 at the PML/non-PML interface to its maximum at the outer boundaries of the computational domain to minimize the numerical reflections caused by spatial discretization. Because the PML parameter optimization issue (Collino and Monk, 1998; Marengo et al., 1999) is beyond the scope of this work, we determine the PML decay factor η empirically using the following expressions:

$$\eta_\alpha(\alpha) = \begin{cases} \eta_m[(L_{pml} - \alpha)/L_{pml}]^3 & \text{for } \alpha \le L_{pml} \\ 0 & \text{for } L_{pml} < \alpha \le L_{pml} + \alpha_m \\ \eta_m[(\alpha - L_{pml} - \alpha_m)/L_{pml}]^3 & \text{for } \alpha \le L_{pml}, \end{cases} \tag{8}$$

where $\alpha \in \{x,y,z\}$, L_{pml} is the thickness of the PML layer, η_m is the maximum PML decay factor, and α_m is the size of the physical medium domain.

According to Cummer (2003), the NPML variant is given by

$$\frac{\partial}{\partial\alpha}\left(\frac{p}{\gamma_\alpha}\right) + j\omega\rho v_\alpha = f_\alpha, \tag{9}$$

$$\frac{\partial}{\partial x}\left(\frac{v_x}{\gamma_x}\right) + \frac{\partial}{\partial y}\left(\frac{v_y}{\gamma_y}\right) + \frac{\partial}{\partial z}\left(\frac{v_z}{\gamma_z}\right) + \frac{1}{\lambda} j\omega p = q, \tag{10}$$

where $\alpha \in \{x,y,z\}$.

Evidently, the above NPML formulation deviates from the standard complex stretched coordinate PML if the decay factor η is spatially variant. However, these two systems are actually equivalent mathematically, which we prove by using a variable substitution technique.

Implementation of NPML

The implementation of the NPML is straightforward and simple. First, we convert equations 9 and 10 to

$$\frac{\partial \bar{p}^\alpha}{\partial\alpha} + j\omega\rho v_\alpha = f_\alpha, \tag{11}$$

$$\frac{\partial \bar{v}_x^x}{\partial x} + \frac{\partial \bar{v}_y^y}{\partial y} + \frac{\partial \bar{v}_z^z}{\partial z} + \frac{1}{\lambda} j\omega p = q, \tag{12}$$

where $\alpha \in \{x,y,z\}$. To complete this system of equations, the regular state variables ξ must be connected to the auxiliary state variables $\bar{\xi}^\alpha$ by coupling the system to the auxiliary ordinary differential equations (ODEs) (after being converted to the time domain):

$$\bar{\xi}^\alpha = \frac{\xi}{1 - j\eta_\alpha/\omega}, \tag{13}$$

where $\xi \in \{p, v_x, v_y, v_z\}$.

Clearly, equations 11 and 12 remain exactly the same form as the original governing equations in the physical medium (see equations 3 and 4). This point demonstrates the simplicity of the implementation of the NPML because there is no need to modify the system of equations when applied to either the regular medium region or the NPML region. The only additional operation required is to solve a few simple auxiliary ODEs. Furthermore, these equations are independent of the finite-difference scheme, which means that the NPML can be coded as general, reusable, and standard subroutines.

In particular, to implement the NPML using the FDTD method, we first need to transfer the frequency-domain scalar equations 11–13 back to the time domain as follows:

$$\frac{\partial \bar{p}^\alpha}{\partial\alpha} + \rho\frac{\partial v_\alpha}{\partial t} = f_\alpha, \tag{14}$$

$$\frac{\partial \bar{v}_x^x}{\partial x} + \frac{\partial \bar{v}_y^y}{\partial y} + \frac{\partial \bar{v}_z^z}{\partial z} + \frac{1}{\lambda}\frac{\partial p}{\partial t} = q, \tag{15}$$

$$\frac{\partial \bar{\xi}^\alpha}{\partial t} + \eta_\alpha \bar{\xi}^\alpha = \frac{\partial \xi}{\partial t}, \tag{16}$$

where $\alpha \in \{x,y,z\}$ and $\xi \in \{p, v_x, v_y, v_z\}$.

Then, after the spatial and temporal discretization, we can use equation 14 to update v_α. With equation 16, we are able to find the auxiliary variables $\bar{v}_\alpha^\alpha$. Finally, the regular state variable p is updated by using equation 15. The last step of the algorithm is to calculate the auxiliary variables $\bar{p}^\alpha$ to prepare for the next FDTD iteration. In total, we need six auxiliary variables ($\bar{p}^x, \bar{p}^y, \bar{p}^z, \bar{v}_x^x, \bar{v}_y^y, \bar{v}_z^z$) and six extra corresponding ODEs to complete the whole system.

MATHEMATICAL ANALYSIS

Advantages of the NPML

As mentioned in the previous section, the first advantage of the NPML is that it is very easy to implement. The second advantage of the NPML is that it does not change the form of the governing equations, which means that the NPML can be applied in different numerical methods without changing the main code (only the NPML auxiliary ODEs change). This fact makes the NPML very flexible and efficient because, in many other practical applications, the derivation of the difference equation coefficients is complicated and tedious. Another important advantage of the NPML is that it saves computational cost in comparison with the standard complex stretched coordinate PML, which is discussed in detail below.

Similarly, the standard complex stretched coordinate PML does not require modification of the original governing equations (Chew and Weedon, 1994). To implement the standard PML without modifying the main code, we need to write equations 5 and 6 as follows by introducing some auxiliary variables:

$$\frac{\partial p}{\partial\alpha} + j\omega\rho\tilde{v}_\alpha^\alpha = f_\alpha, \tag{17}$$

$$\frac{\partial \tilde{\tilde{v}}_x^{yz}}{\partial x} + \frac{\partial \tilde{\tilde{v}}_y^{xz}}{\partial y} + \frac{\partial \tilde{\tilde{v}}_z^{xy}}{\partial z} + \frac{1}{\lambda} j\omega \tilde{\tilde{\tilde{p}}}^{xyz} = q, \tag{18}$$

where $\tilde{\xi}^\alpha = \xi(1 - j\eta_\alpha/\omega)$. The multiple tildes denote the multiple multiplications by the stretched coordinate factors $(1 - j\eta_\alpha/\omega)$ and the superscripts represent the directions of the stretched coordinate factors. For example, $\tilde{\tilde{v}}_x^{yz} = v_x(1 - j\eta_y/\omega)(1 - j\eta_z/\omega)$.

At the first look, there is no fundamental difference between the systems (equations 11 and 12 and 17 and 18). However, to solve equations 17 and 18, we need 12 auxiliary variables because of the multiple complex coordinate stretching in the equations. As a result, 12 additional ODEs have to be included in the system, even though there are only seven auxiliary state variables ($\tilde{v}_x^x, \tilde{v}_y^y, \tilde{v}_z^z, \tilde{\tilde{v}}_x^{yz}, \tilde{\tilde{v}}_y^{xz}, \tilde{\tilde{v}}_z^{xy}, \tilde{\tilde{\tilde{p}}}^{xyz}$) explicitly appearing in equations17 and 18.

Consequently, in acoustic wave propagation modeling, the replacement of the standard complex stretched coordinate PML by the

NPML results in higher computational efficiency without loss of accuracy, simplicity, or generality, which is shown through mathematical analysis and numerical experiments presented in the remainder of this paper. We have to mention that some PML formulations use even fewer auxiliary state variables and fewer additional equations (Roden and Gedney, 2000). However, these formulations change the form of the original governing equations, which increases the computational complexity in practical problems. Therefore, in this work, we only compare the NPML with the standard complex stretched coordinate PML because both of them maintain the form of the original governing equations.

In addition, the NPML is a general PML. It can be applied to any linear medium, which can be inhomogeneous, anisotropic, dispersive, or lossy, and it is very straightforward to apply the NPML in cylindrical and spherical coordinates (Hu and Cummer, 2006).

NPML is a true PML

The standard complex stretched coordinate PML formulation and the NPML formulation are identical only if the decay factor η is spatially invariant, which is not true in most applications. Hu and Cummer (2004) theoretically proved that these two formulations are fundamentally identical in 2D Cartesian coordinates for electromagnetic wave propagations, even if the PML parameters are spatially variant. In this work, we prove that this conclusion remains valid in 3D Cartesian coordinates for acoustic wave propagation problems.

First, we divide both sides of equation 10 by $\Gamma = \gamma_x\gamma_y\gamma_z$ to obtain

$$\frac{\partial}{\Gamma\partial x}\left(\frac{v_x}{\gamma_x}\right) + \frac{\partial}{\Gamma\partial y}\left(\frac{v_y}{\gamma_y}\right) + \frac{\partial}{\Gamma\partial z}\left(\frac{v_z}{\gamma_z}\right) + \frac{1}{\lambda}j\omega\frac{p}{\Gamma} = q. \tag{19}$$

Then, because γ_α is only α-variant, we can rearrange the equation as follows:

$$\frac{\partial}{\gamma_x\partial x}\left(\frac{v_x}{\Gamma}\right) + \frac{\partial}{\gamma_y\partial y}\left(\frac{v_y}{\Gamma}\right) + \frac{\partial}{\gamma_z\partial z}\left(\frac{v_z}{\Gamma}\right) + \frac{1}{\lambda}j\omega\left(\frac{p}{\Gamma}\right) = q, \tag{20}$$

which can be written as

$$\frac{\partial\tilde{\tilde{\tilde{v}}}_x^{xyz}}{\gamma_x\partial x} + \frac{\partial\tilde{\tilde{\tilde{v}}}_y^{xyz}}{\gamma_y\partial y} + \frac{\partial\tilde{\tilde{\tilde{v}}}_z^{xyz}}{\gamma_z\partial z} + \frac{1}{\lambda}j\omega\tilde{\tilde{\tilde{p}}}^{xyz} = q, \tag{21}$$

where $\tilde{\tilde{\tilde{\xi}}}^{xyz} = \frac{\xi}{\gamma_x\gamma_y\gamma_z} = \frac{\xi}{\Gamma}$. On the right side of equations 19–21, the factor $\frac{1}{\Gamma}$ is removed because the monopole sources are always located in non-PML regions, where $\Gamma \equiv 1$.

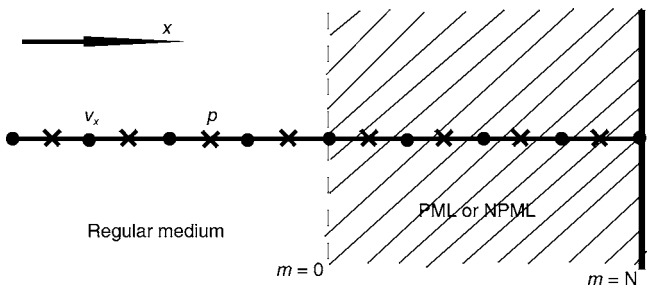

Figure 1. The diagram of the 1D acoustic P-wave propagation in the $+x$ direction through the PML/NPML layer. The field p is defined at $x = (m + 1/2)\Delta x$ and v_x is defined at $x = m\Delta x$, where m is an integer.

Similarly, we can transfer equation 9 to

$$\frac{\partial\tilde{\tilde{\tilde{p}}}^{xyz}}{\gamma_\alpha\partial\alpha} + j\omega\rho\tilde{\tilde{\tilde{v}}}_\alpha^{xyz} = f_\alpha, \tag{22}$$

where $\alpha \in \{x, y, z\}$.

The new NPML system (equations 21 and 22) is in exactly the same form as the standard PML system (equations 5 and 6) except that the regular state variables ξ in the standard PML formulations are replaced by the auxiliary state variables $\tilde{\tilde{\tilde{\xi}}}^{xyz}$ in the NPML formulations. This proves that these two PML formulations are mathematically equivalent in the physical medium region because the auxiliary state variables are equivalent to the regular state variables in the physical medium domain where the PML/NPML decay factor η is equal to zero.

However, the wave behaviors are different for these two formulations in the PML/NPML regions because of variable change scheme employed in the NPML formulation. The regular state variables ξ in the standard PML are continuous across the interface between the PML region and the physical medium region. However, in the NPML formulation, the auxiliary state variables, instead of the regular state variables $\tilde{\tilde{\tilde{\xi}}}^{xyz}$, are continuous across the interface. To make this point clear, we regard the NPML as the complex stretched field PML because, in the NPML, it is the field instead of the coordinate that is stretched by a complex factor.

Numerical reflection analysis

Although we have proved that the NPML and the standard PML are analytically equivalent, for optimization purpose, we still need to investigate their performance after spatial discretization. For simplicity, here we consider only a simple 1D case for the theoretical numerical reflection analysis.

As shown in Figure 1, we assume there is a P-wave propagating in the $+x$ direction in a source-free region and there is no y and z variation. With the spatial discretization scheme we employed, the field p is defined at $x = (m + \frac{1}{2})\Delta x$ (labeled by $\times$) and v_x is defined at $m\Delta x$ (labeled by $\bullet$), where m is an integer. The PML/NPML region is between $x = 0$ and $x = N\Delta x$, where N is the number of the grids in the PML/NPML region and Δx is the grid size. For this 1D configuration, the standard PML formulation can be simplified to

$$\frac{\partial p}{\partial x} + j\omega\rho\gamma_x v_x = 0, \tag{23}$$

$$\frac{\partial v_x}{\partial x} + j\omega\frac{\rho}{\lambda}\gamma_x p = 0. \tag{24}$$

For example, if we use a second-order spatial finite difference approach, we obtain the following equations from equation 24:

$$p\big|_{m+\frac{1}{2}} = -\frac{\lambda_{m+\frac{1}{2}}}{j\omega\rho_{m+\frac{1}{2}}\gamma_{m+\frac{1}{2}}}\frac{v_x\big|_{m+1} - v_x\big|_m}{\Delta x}, \tag{25}$$

$$p|_{m-\frac{1}{2}} = -\frac{\lambda_{m-\frac{1}{2}}}{j\omega\rho_{m-\frac{1}{2}}\gamma_{m-\frac{1}{2}}}\frac{v_x|_m - v_x|_{m-1}}{\Delta x}, \quad (26)$$

where $\xi|_m = \xi(x = m\Delta x)$ and $\gamma_m = \gamma_x(x = m\Delta x)$. Similarly, discretizing equation 23, we have

$$j\omega\rho_m\gamma_m v_x|_m = -\frac{p|_{m+\frac{1}{2}} - p|_{m-\frac{1}{2}}}{\Delta x}. \quad (27)$$

Substituting equations 25 and 26 into equation 27, we have

$$\left(\omega^2\rho_m\gamma_m\Delta x^2 - \frac{\lambda_{m+\frac{1}{2}}}{\rho_{m+\frac{1}{2}}\gamma_{m+\frac{1}{2}}} - \frac{\lambda_{m-\frac{1}{2}}}{\rho_{m-\frac{1}{2}}\gamma_{m-\frac{1}{2}}}\right)v_x|_m + \frac{\lambda_{m+\frac{1}{2}}}{\rho_{m+\frac{1}{2}}\gamma_{m+\frac{1}{2}}}v_x|_{m+1} + \frac{\lambda_{m-\frac{1}{2}}}{\rho_{m-\frac{1}{2}}\gamma_{m-\frac{1}{2}}}v_x|_{m-1} = 0, \quad (28)$$

which describes the relation between the adjacent points in the whole computational domain. By letting $m = 0, 1, \ldots, N-1$, we can obtain a system consisting of N linear equations. Combined with the Dirichlet boundary condition at the rightmost boundary, these equations can be written in the matrix form and enable us to calculate the numerical reflection coefficients analytically (Collino and Monk, 1998). In this work, because our goal is to find whether the standard PML and the NPML have identical numerical reflection coefficients, it is not necessary to write the numerical reflection coefficients in closed form.

Similarly, for the NPML, the field values at the adjacent nodes are related by

$$\left(\omega^2\rho_m\Delta x^2 - \frac{\lambda_{m+\frac{1}{2}}}{\rho_{m+\frac{1}{2}}\gamma_{m+\frac{1}{2}}\gamma_m} - \frac{\lambda_{m-\frac{1}{2}}}{\rho_{m-\frac{1}{2}}\gamma_{m-\frac{1}{2}}\gamma_m}\right)v_x|_m + \frac{\lambda_{m+\frac{1}{2}}}{\rho_{m+\frac{1}{2}}\gamma_{m+\frac{1}{2}}\gamma_{m+1}}v_x|_{m+1} + \frac{\lambda_{m-\frac{1}{2}}}{\rho_{m-\frac{1}{2}}\gamma_{m-\frac{1}{2}}\gamma_{m-1}}v_x|_{m-1} = 0, \quad (29)$$

which is different from equation 28. However, noticing that in the NPML, because of the variable change scheme, it is the auxiliary state variable $\bar{\xi}^{\alpha}$ that is continuous across the NPML/non-NPML interface, we can rewrite equation 29 as

$$\left(\omega^2\rho_m\gamma_m\Delta x^2 - \frac{\lambda_{m+\frac{1}{2}}}{\rho_{m+\frac{1}{2}}\gamma_{m+\frac{1}{2}}} - \frac{\lambda_{m-\frac{1}{2}}}{\rho_{m-\frac{1}{2}}\gamma_{m-\frac{1}{2}}}\right)\bar{v}_x^x|_m + \frac{\lambda_{m+\frac{1}{2}}}{\rho_{m+\frac{1}{2}}\gamma_{m+\frac{1}{2}}}\bar{v}_x^x|_{m+1} + \frac{\lambda_{m-\frac{1}{2}}}{\rho_{m-\frac{1}{2}}\gamma_{m-\frac{1}{2}}}\bar{v}_x^x|_{m-1} = 0. \quad (30)$$

Evidently, because all the auxiliary variables are equivalent to the regular variables in the physical medium region, equation 30 must yield the same numerical reflection coefficient as equation 28. In other words, the NPML is equivalent to the standard complex stretched coordinate PML also after the spatial discretization. However, this is not necessarily true in cylindrical or spherical coordinates.

NUMERICAL SIMULATIONS

The purpose of the first example is to compare the wave-absorbing performance between the standard PML and the NPML. The geometry of this numerical simulation is shown in Figure 2. This example is depicted in Abubakar et al. (2003). The truncated domain size is 610 m in the x-direction and 400 m in the z-direction. In this simulation, we use the same grid size in the x- and z-directions ($\Delta x = \Delta z = 10$ m). This truncated domain is surrounded by a 30-grid-thick PML/NPML layer. The monopole source located at (315 m, 45 m) is a Ricker wavelet with the dominant frequency at 12.5 Hz. There are five types of materials presented in the computational domain, whose P-wave velocities are 2250, 1500, 2100, 2500, and 3000 m/s, respectively. Although the mass density can be inhomogeneous, for convenience, it is assumed to be constant everywhere (2500 kg/m^3) in this example.

In this numerical experiment, we use a fourth-order spatial finite-difference and a second-order temporal finite-difference scheme (Fang, 1989; Shlager, 2003). The received P-waves at the leftmost receiver (5 m, 45 m), which is a half grid point away from the PML/non-PML interface, are plotted in Figure 3a, where the reference solution is obtained by running the FDTD code without any absorbing boundary condition in a very large extended computational domain designed to ensure that there is no reflected wave arriving at the receiver at the end of the simulation. Figure 3b shows the artificial reflections recorded at the receiver introduced by the standard PML and the NPML, i.e., the difference between the reference solution and the solutions with the standard PML or the NPML. The wave-absorbing rate is above 70 dB for all the frequencies in this example. If we adjust the thickness of the PML/NPML layers and the decay factor, the absorbing rate can be higher. As expected by the preceding theoretical analysis, the difference between the standard PML solution and the NPML solution is simply the accumulated double precision truncation error shown in Figure 3c. In this example, the standard PML employed six auxiliary variables and the corresponding extra ODEs, while the NPML only uses four. On a PC with a 2.40-GHz processor, the simulation using the standard PML takes

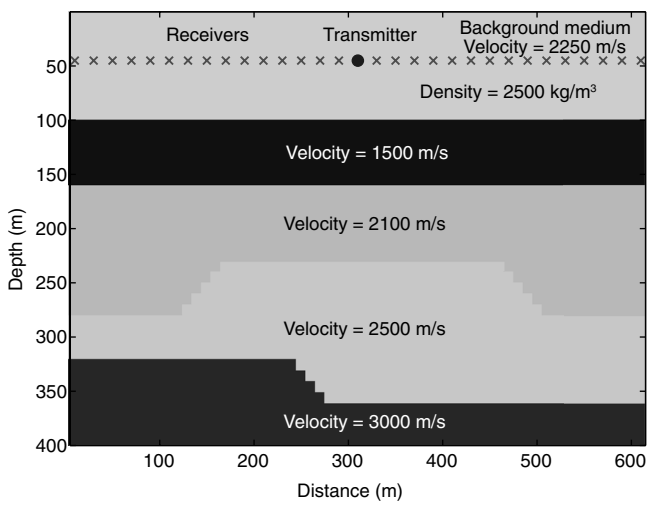

Figure 2. The geometry of the first numerical experiment. The mass density is assumed to be constant (2500 kg/m^3) everywhere. The test domain shown here is surrounded by the PML/NPML layers (not shown in the figure), whose properties are extended from the test domain.

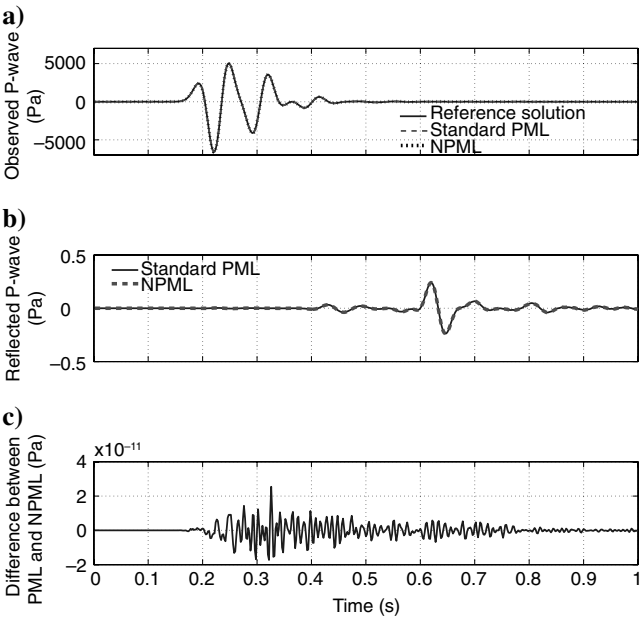

Figure 3. The received P-waves at (5 m, 45 m) and the artificially reflected waves caused by the standard PML and the NPML. (a) The reference solution, the solution using the standard PML, and the solution using the NPML. (b) The reflected P-wave, i.e., the differences between the reference solution and the solution using the standard PML or the NPML. (c) The difference between the solutions using the standard PML and the NPML.

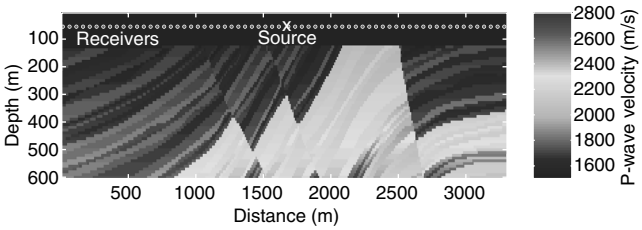

Figure 4. The Marmousi velocity model and the distribution of the monopole source and the receivers.

approximately 8.3 s, although the simulation using the NPML takes only 6.9 s. The latter reduces the computation time by 17%. In 3D applications, because the NPML uses only half the number of the auxiliary variables and extra ODEs compared with the standard PML approach, the computation time and memory saving obviously can be more significant.

To further investigate the NPML performance, we conducted another numerical simulation in a more complicated structure, the Marmousi velocity model, as shown in Figure 4, where the monopole source and the receivers are indicated by the cross ($\times$) and the dots ($\bullet$), respectively. In this simulation, we use a Ricker wavelet at (1665 m, 55 m). Again, the reference solution is obtained by running the code in a large extended computational domain. To carefully quantify the wave-absorbing rate of the NPML used in the Marmousi velocity model, we plot the time waveform of the received pressure field at the leftmost receiver (35 m, 55 m) in Figure 5a. Figure 5b shows the artificially reflected wave at the above-specified receiver (the difference between the reference solution and the solution using the NPML). The frequency spectrum of this artificial reflection shown in Figure 5c indicates that the wave-absorbing rate of the NPML in such a complicated structure is still above 70 dB. The results are similar at the other receivers shown in Figure 4.

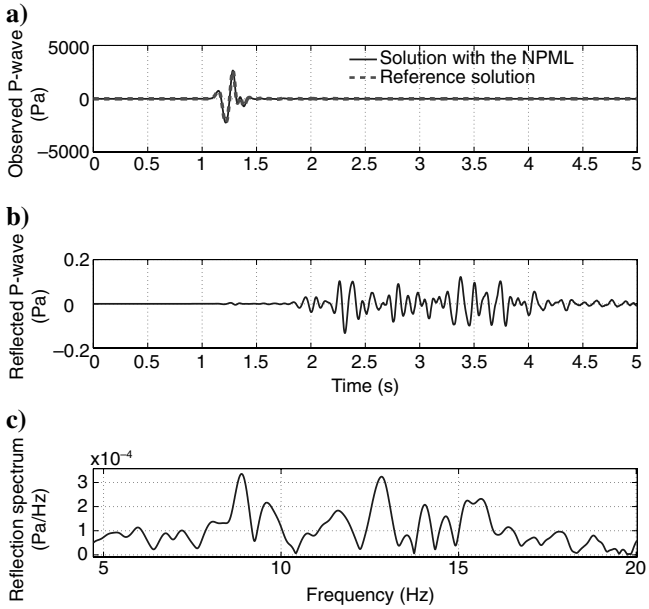

Figure 5. The simulation results on the NPML performance testing in the Marmousi velocity model. (a) The received P-waves at the receiver located at (35 m, 55 m) in the Marmousi velocity model shown in Figure 4. (b) The artificially reflected P-wave at the receiver located at (35 m, 55 m), i.e., the difference between the reference solution and the solution using the NPML. (c) The frequency spectrum of the artificial reflection.

CONCLUSION

In this work, a recently developed perfectly matched layer known as NPML was applied to acoustic wave propagation modeling. The NPML simplifies the implementation of the absorbing boundary condition in complicated structures and media without losing exactness and performance. Furthermore, the NPML has some valuable advantages over other PML formulations. Compared with the standard complex stretched coordinate PML, the NPML is more computationally efficient. For the 2D example presented in this work, the computation time saving is up to 17%. For 3D problems or more complicated applications, the replacement of the standard PML by the NPML can significantly save the computation operations and the physical memory use.

By rigorously analyzing the NPML properties, we proved that the NPML is mathematically equivalent to the standard PML in 3D Cartesian coordinates for acoustic wave propagation modeling in spite of the inexact variable change scheme employed by the NPML. Moreover, the wave-absorbing performance of these two PML formulations is identical even after spatial discretization, which has been validated through the numerical simulation results presented.

Although the examples considered in this work are simple media, the NPML is intrinsically a general PML, which can be applied to any linear medium with complicated properties (dispersive, lossy, inhomogeneous, and anisotropic).

ACKNOWLEDGMENTS

The authors acknowledge the helpful comments from Kees Wapenaar, Brackin Smith, and an anonymous reviewer that greatly improved this manuscript.

REFERENCES

Abubakar, A., P. M. van den Berg, and J. T. Fokkema, 2003, Towards non-linear inversion for characterization of time-lapse phenomena through numerical modelling: Geophysical Prospecting, **51**, 285–293.

Bérenger, J. P., 1994, A perfectly matched layer for the absorption of electromagnetic waves: Journal of Computational Physics, **114**, 185–200.

———, 1996, Three-dimensional perfectly matched layer for the absorption of electromagnetic waves: Journal of Computational Physics, **127**, 363–379.

———, 2004, On the reflection from Cummer's nearly perfectly matched layer: IEEE Microwave and Wireless Components Letters, **14**, 334–336.

Chew, W. C., and W. H. Weedon, 1994, A 3D perfectly matched medium from modified Maxwell's equations with stretched coordinates: IEEE Transactions on Antennas and Propagation, **43**, 599–604.

Collino, F., and P. B. Monk, 1998, Optimizing the perfectly matched layer: Computer Methods in Applied Mechanics and Engineering, **164**, 157–171.

Cummer, S. A., 2003, A simple, nearly perfectly matched layer for general electromagnetic media: IEEE Microwave and Wireless Components Letters, **13**, 137–140.

———, 2004, Perfectly matched layer behavior in negative refractive index materials: IEEE Antennas and Wireless Propagation Letters, **3**, 172–175.

Engquist, B., and A. Majda, 1977, Absorbing boundary conditions for the numerical simulation of waves: Mathematics of Computation, **31**, 629–651.

Fang, J., 1989, Time domain finite difference computation for Maxwell's equations: Ph.D. thesis, University of California, Berkeley.

Fokkema, J. T., and P. M. van den Berg, 1993, Seismic applications of acoustic reciprocity: Elsevier Science Pub. Co., Inc.

Gedney, S. D., 1996, An anisotropic PML absorbing media for the FDTD simulation of fields in lossy and dispersive media: Electromagnetics, **16**, 399–415.

Hu, W., and S. A. Cummer, 2004, The nearly perfectly matched layer is a perfectly matched layer: IEEE Antennas and Wireless Propagation Letters, **3**, 137–140.

———, 2006, An FDTD model for low and high altitude lightning-generated EM fields: IEEE Transactions on Antennas and Propagation, **54**, 1513–1522.

Katz, D. S., E. T. Thiele, and A. Taflove, 1994, Validation and extension to three dimensions of the Bérenger absorbing boundary condition for FDTD meshes: IEEE Microwave Guided Wave Letters, **4**, 268–270.

Marengo, E. A., C. M. Rappaport, and E. L. Miller, 1999, Optimum PML ABC conductivity profile in FDFD: IEEE Transactions on Magnetics, **35**, 1506–1509.

Mur, G., 1981, Absorbing boundary conditions for the finite-difference approximation of the time-domain electromagnetic field equations: IEEE Transactions on Electromagnetic Compatability, **EMC-23**, 377–382.

Ramadan, O., 2005, Unconditionally stable nearly PML algorithm for linear dispersive media: IEEE Microwave and Wireless Components Letters, **15**, 490–492.

Roden, J. A., and S. D. Gedney, 2000, Convolutional PML (CPML): an efficient FDTD implementation of the CFS-PML for arbitrary media: Microwave and Optical Technology Letters, **27**, 334–339.

Sacks, Z. S., D. M. Kingsland, R. Lee, and J. F. Lee, 1995, A perfectly matched anisotropic absorber for use as an absorbing boundary condition: IEEE Transactions on Antennas and Propagation, **43**, 1460–1463.

Shlager, K. L., 2003, Comparison of the dispersion properties of several low-dispersion finite-difference time-domain algorithms: IEEE Transactions on Antennas and Propagation, 51, 642–653.